

Seasonal variability in phytoplankton stable carbon isotope ratios and bacterial carbon sources in a shallow Dutch lake

J. M. Lammers,¹ G. J. Reichart,^{1,2} J. J. Middelburg ^{1*}

¹Faculty of Geosciences, Department of Earth Sciences, Utrecht University, Utrecht, The Netherlands

²Department of Ocean Systems, NIOZ Royal Netherlands Institute for Sea Research, Den Burg, Texel, The Netherlands

Abstract

Ecosystem metabolism of lakes strongly depends on the relative importance of local vs. allochthonous carbon sources and on microbial food-web functioning and structure. Over the year ecosystem metabolism varies as a result of seasonal changes in environmental parameters such as nutrient levels, light, temperature, and variability in the food web. This is reflected in isotopic compositions of phytoplankton and bacteria. Here, we present the results of a 17-month study on carbon dynamics in two basins of Lake Naarden, The Netherlands. One basin was restored after anthropogenic eutrophication, whereas the other basin remained eutrophic. We analyzed natural stable carbon isotope abundances ($\delta^{13}\text{C}$) of dissolved inorganic carbon, dissolved organic carbon and macrophytes, and combined these data with compound-specific $\delta^{13}\text{C}$ analyses of phospholipid-derived fatty acids, produced by phytoplankton and bacteria. Isotopic fractionation (ϵ) between phytoplankton biomass and $\text{CO}_{2(\text{aq})}$ was similar for diatoms and other eukaryotic phytoplankton, and differences between sampling sites were small. Highest ϵ values were observed in winter with values of $23.5 \pm 0.6\text{‰}$ for eukaryotic phytoplankton and $13.6 \pm 0.3\text{‰}$ for cyanobacteria. Lowest ϵ values were observed in summer: $10.5 \pm 0.3\text{‰}$ for eukaryotic phytoplankton and $2.7 \pm 0.1\text{‰}$ for cyanobacteria. The annual range in $\delta^{13}\text{C}_{\text{bact}}$ was between 6.9‰ and 8.2‰ for the restored and eutrophic basin, respectively, while this range was between 11.6‰ and 13.1‰ for phytoplankton in the restored and eutrophic basin, respectively. Correlations between $\delta^{13}\text{C}_{\text{phyto}}$ and $\delta^{13}\text{C}_{\text{bact}}$ were strong at both sites. During summer and fall, bacterial biomass derives mainly from locally produced organic matter, with minor allochthonous contributions. Conversely, during winter, bacterial dependence on allochthonous carbon was 39–77% at the restored site, and 17–46% at the eutrophic site.

Freshwater systems play an important role in the global carbon cycle despite their limited spatial extent. Inland waters process large amounts of carbon (Cole et al. 2007; Battin et al. 2008; Tranvik et al. 2009) and, compared to oceans, have a disproportionately high storage capacity resulting from high production rates and high sedimentation rates. Nevertheless, the surface waters of lakes are often supersaturated with respect to CO_2 (Cole et al., 1994), resulting in emission of CO_2 to the atmosphere. Although dissolved inorganic carbon (DIC) loading from the watershed may be a cause (McDonald et al., 2013), the imbalance between lacustrine and atmospheric partial pressures of CO_2 often results from excess respiration compared to primary production. The carbon supporting

respiration can be derived from either autochthonous (locally produced) or allochthonous (external inputs from plants and soils) sources. Ecosystem metabolism and net impact on the global carbon cycle strongly depend on the relative importance of these carbon sources and hence microbial food web functioning and structure.

The microbial food web is not only affected by input of allochthonous organic matter but also by environmental parameters such as nutrient levels, temperature, and light availability, which influence primary productivity. Even though all these factors vary strongly throughout the year, microbial food-web studies are usually snapshots representing days (Staeher and Sand-Jensen 2007; Staeher et al. 2010; Coloso et al. 2011) to weeks (Cole et al. 1988; Pace et al. 2004; Cole et al. 2006; Brett et al. 2009; De Kluijver et al. 2010) because of limitations in time and resources. Studies on the effects of seasonal variability on carbon processing and the microbial food web hence are relatively scarce. The few studies of seasonal changes in phytoplankton carbon isotopic composition generally show large variability (Finlay 2004; Bontes et al. 2006; Van Breugel et al. 2006; De Kluijver et al. 2015), resulting from

*Correspondence: j.b.m.middelburg@uu.nl

Additional Supporting Information may be found in the online version of this article.

This is an open access article under the terms of the Creative Commons Attribution License, which permits use, distribution and reproduction in any medium, provided the original work is properly cited.

changes in growth rate and carbonate chemistry (pH, $p\text{CO}_2$). Also seasonal variability in the dependence of zooplankton on allochthonous carbon via microbial links has been reported (Grey and Jones 2001; Van den Meersche et al. 2009).

In the past, stable carbon isotopes have been applied to trace energy flow at higher food-web levels (e.g., Peterson and Fry 1987; Kling et al. 1992; Keough et al. 1996). A major challenge however, has been to distinguish between organisms at the base of the food web (phytoplankton, bacteria) and particulate organic carbon (POC) (Middelburg, 2014). Indirect measurements such as different size classes of POC and their carbon isotopic compositions have been used to infer the $\delta^{13}\text{C}$ of phytoplankton (Marty and Planas 2008). However, these size-based approaches are difficult to apply in turbid, eutrophic systems and estimations from DIC involve large uncertainties in terms of fractionation and correction factors (Middelburg 2014; Taipale et al. 2015). Compound-specific stable isotope analyses nowadays allow addressing different components of the food web, including the base (Boschker et al. 1998; Middelburg et al. 2000; Van den Meersche et al. 2009). Especially phospholipid-derived fatty acids (PLFAs), components of cell membranes, are excellently suited for natural abundance isotope studies since they are hydrolyzed within hours to days after cell death (White et al. 1979; Harvey et al. 1986) and thus represent freshly produced biomass. PLFAs are produced by a large variety of organisms and although they do not represent unique organisms, they can be used to differentiate between phytoplankton (eukaryotic algae, prokaryotic cyanobacteria) and heterotrophic bacteria (Kaneda 1991; Boschker and Middelburg 2002; Gugger et al. 2002; Dijkman and Kromkamp 2006; Taipale et al. 2013). Accordingly, PLFAs have been successfully applied to food-web studies (Rütters et al. 2002), including in lakes (Bontes et al. 2006; Pace et al. 2007; De Kluijver et al. 2014).

Here, we investigate phytoplankton-bacteria coupling over a 17-month period in two basins of successfully restored Lake Naarden (Naardermeer), The Netherlands. Lake Naarden is a shallow (~ 1 m water depth) wetland lake, lying within the Naardermeer nature reserve. The lake has a surface area of 1042 ha and consists of five connected basins and canals that are surrounded by marshy woodland, open reed-marshland, and meadows (Fig. 1). Until the 1960s, water was supplemented by rainfall, groundwater discharge and water levels were maintained by pumping water to and from the river Vecht. Water supply from the river Vecht was stopped after 1960 because of eutrophication of this water. Nevertheless, eutrophication of Naardermeer continued after 1960, with increasing turbidity and decreasing aquatic vegetation (mostly charophytes and *Najas marina*). Original macrophyte vegetation gave way to species associated with eutrophication and seasonal algal blooms (Bootsma et al. 1999). A restoration project started in 1985 aiming at reducing the P-load by supplying phosphate-free water. After a decade turbidity was reduced and macrophytes had largely recovered in most of

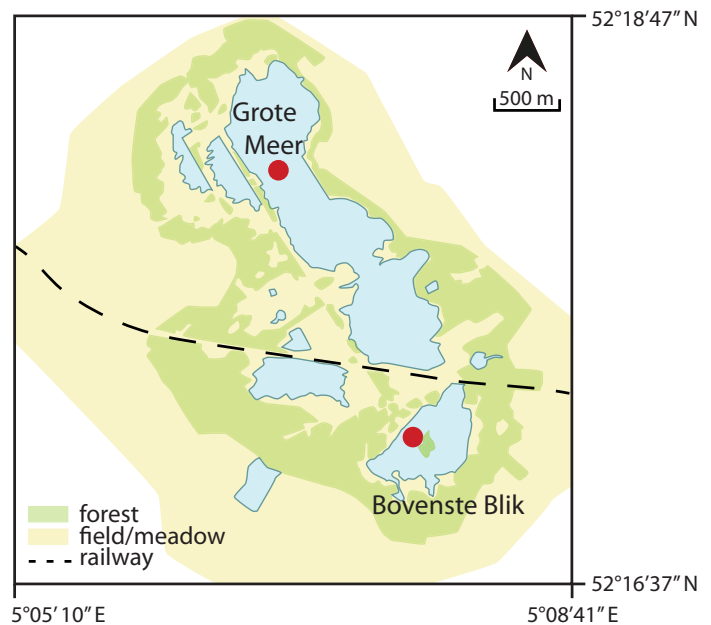


Fig. 1. Map of Lake Naarden and the surrounding vegetation types. Samples were taken in two basins: GM and BB. Sampling locations are indicated by red circles.

the lake (Bootsma et al. 1999). Currently, dephosphorized water is supplied from the river Vecht in dry periods (summer), but only reaches the area north of the railway (Fig. 1). Diatom studies have shown that water quality has recovered in particular north of the railway. The northern basin Grote Meer (GM) (Fig. 1) is considered of “very good” quality, with Secchi depths, ranging from ~ 0.8 m in summer to ~ 1.2 m in winter (water depth ~ 1.2 m). Chlorophyll *a* concentrations between $6 \mu\text{g L}^{-1}$ and $31 \mu\text{g L}^{-1}$ suggest meso- to eutrophic conditions, while average total phosphorous (TP) concentration of $29 \mu\text{g P L}^{-1}$ (ranging between $< 10 \mu\text{g P L}^{-1}$ and $60 \mu\text{g P L}^{-1}$) are indicative of eutrophic conditions. Bovenste Blik (BB) south of the railway is still moderately disturbed (Van Ee 2007). This is also reflected in Secchi depths ranging between 0.4 m and 0.8 m (water depth ~ 1 m). In this basin, Chl *a* concentrations between $14 \mu\text{g L}^{-1}$ and $87 \mu\text{g L}^{-1}$ are indicative of eutrophic conditions and also TP concentrations are higher compared to site GM, ranging between $20 \mu\text{g P L}^{-1}$ and $160 \mu\text{g P L}^{-1}$ (average of $65 \mu\text{g P L}^{-1}$) during our sampling year.

This study addresses seasonal changes in phytoplankton isotopes and carbon transfer to bacteria using stable isotope analyses of inorganic (DIC) and organic (dissolved organic carbon [DOC] and aquatic and terrestrial vegetation) carbon as well as compound-specific stable carbon isotope analyses of phytoplankton and bacteria via PLFAs. We examine bacterial dependence on autochthonous vs. allochthonous carbon sources throughout the year. We compare the results from the two basins of Lake Naarden, aiming to improve understanding of the effects of trophic state.

Material and methods

Sample collection

Between May 2013 and September 2014, water was collected monthly from two basins of Lake Naarden: GM and BB (Fig. 1). Ten liters of water were transported to the laboratory and sampled for DIC, DOC, and suspended particulate matter (SPM). Samples for DIC and DOC carbon isotopic composition were filtered through 0.45 μm GF/F filters. DIC samples were collected air-free in 20 mL headspace vials, which were sealed airtight, poisoned using mercury chloride, and subsequently stored dark and upside down. After filtering, DOC samples were stored frozen (-20°C) until analysis. Remaining water was filtered for SPM using pre-weighed and pre-combusted GF/F filters (0.7 μm) and frozen (-20°C) until extraction. Aquatic, littoral, and terrestrial vegetation was collected in September 2015 and stored frozen until further analyses.

Data on temperatures, Chl *a* concentrations, pH values, and concentrations of carbonate species were collected and kindly provided by water company Waternet and its associated laboratory Waterproef, commissioned by Natuurmonumenten, the Society for preservation of nature monuments in The Netherlands.

Laboratory analyses

DIC concentrations were measured on a Shimadzu TOC-5050A carbon analyzer and calibrated using an in-house seawater standard. Standard deviations were better than 0.3 mg L^{-1} . For $\delta^{13}\text{C}$ analyses, first a helium headspace was generated and DIC samples were then acidified using H_3PO_4 , creating CO_2 -gas of which the $\delta^{13}\text{C}$ values were measured using a gas bench coupled on line to an isotope ratio mass spectrometry (IRMS; Thermo Delta V advantage). Values were calibrated to the Vienna Pee Dee Belemnite (V-PDB) scale using Li_2CO_3 and Na_2CO_3 as standards.

DOC samples were treated and analyzed for $\delta^{13}\text{C}$ following (Boschker et al. 2008), using high-performance liquid chromatography-isotope ratio mass spectrometry (Thermo Surveyor system coupled to a Delta V Advantage using the LC-Isolink interface), using certified reference materials glutamic acid and sucrose for calibration.

POC concentrations and $\delta^{13}\text{C}_{\text{POC}}$ were measured on small pieces (eight circles, 5 mm diameter) cut from the filters collected for SPM analyses. POC concentrations were measured using an elemental analyzer (Fisons Instruments NA1500), coupled online to an IRMS (Thermo Deltaplus) for $\delta^{13}\text{C}$ analyses. Precision for $\delta^{13}\text{C}$ was better than 0.1‰ based on an (in-house) Graphite quartzite standard and 0.2‰ based on an (in-house) Nicotinamide standard. Concentrations were relatively low and hence did not allow for duplicate measurements, still, the observed trends are consistent and confirm that the internal precision is representative.

Vegetation samples were freeze dried and ground to a powder. Carbon isotopic compositions were measured on the same setup described above for analyses of POC.

Standard deviations were better than 0.4‰ based on an in-house graphite quartzite standard.

A modified Bligh and Dyer extraction method was used to extract lipids from freeze-dried SPM samples, which were then separated based on polarity into simple lipid, glycolipid, and PL fractions (Dickson et al. 2009). Subsequently, mild alkaline transmethylation converted phospholipid-derived fatty acids to fatty acid methyl esters (PL-FAMES) (White et al. 1979) and $\text{C}_{12:0}$ and $\text{C}_{19:0}$ FAMES were added as internal standards. Concentrations of PL-FAMES were analyzed using a gas chromatograph (HP 6890) with Helium as carrier gas set at constant pressure and fitted with a flame ionization detector (FID) and a VF-23ms column (0.25 mm internal diameter). Compounds were identified based on retention times and mass spectra following mass spectrometry, which was performed using a Thermo Trace GC Ultra, with Helium set at constant flow. Double-bond positions were determined after derivatization with dimethyl-disulfide (DMDS). DMDS was activated with iodine in diethyl ether at 40°C overnight (Buser et al. 1983). Compound-specific $\delta^{13}\text{C}$ analysis was done using gas chromatography combustion isotope ratio mass spectrometry (GC-C-IRMS) on a Thermo-Finnigan Delta Plus XP using the same type of column that was used during GC-FID analyses. Oven programming of GC-FID, gas chromatography mass spectrometry (GC-MS) and GC-C-IRMS followed Middelburg et al. (2000). Carbon isotopic values of PLFAs are reported in ‰ vs. V-PDB. These were corrected for the carbon atom that was added during methylation. Carbon isotopic values of the derivatizing agents were determined offline (Sessions, 2006).

PLFA assignments

Main PLFAs detected in SPM samples from both sites were branched PLFAs $\text{iC}_{14:0}$, $\text{iC}_{15:0}$, $\text{aC}_{15:0}$, and polyunsaturated fatty acids (PUFAs) $\text{C}_{16:2\omega 7}$, $\text{C}_{18:3\omega 3}$, $\text{C}_{18:4\omega 3}$, $\text{C}_{20:4\omega 6}$, $\text{C}_{20:5\omega 3}$, and $\text{C}_{22:6\omega 3}$. Branched PLFAs $\text{iC}_{14:0}$, $\text{iC}_{15:0}$, and $\text{aC}_{15:0}$ are predominantly produced by gram-positive bacteria (Kaneda 1991) but have also been detected in some gram-negative bacteria (Haack et al. 1994). PUFAs are synthesized by phytoplankton groups, including green and red algae, diatoms, dinoflagellates, and haptophytes (Brett and Müller-Navarra 1997; Dijkman and Kromkamp 2006; Taipale et al. 2013). Detected PUFAs $\text{C}_{18:3\omega 3}$, $\text{C}_{18:4\omega 3}$, $\text{C}_{20:4\omega 6}$, and $\text{C}_{22:6\omega 3}$ derive from numerous phytoplankton groups while PUFAs $\text{C}_{16:2\omega 7}$ and $\text{C}_{20:5\omega 3}$ derive more uniquely from diatoms (Dijkman and Kromkamp 2006). An overview of cell counts for phytoplankton phyla during the summer of 2014 is given in Supporting Information Table S4.

PLFA $\text{C}_{18:3\omega 6}$, which can be used to represent cyanobacteria (Gugger et al. 2002), was found in very low concentrations and only during 4 months at sampling location GM and was not included in the results. At location BB however, $\text{C}_{18:3\omega 6}$ was detected during 11 out of 17 months and concentrations allowed for $\delta^{13}\text{C}$ analyses. Cyanobacterial species

identified in BB include, e.g., the genus *Anabaena*, which is known to produce PLFA C18:3 ω 6 (Gugger et al. 2002). This species was not detected in GM (data not shown), although other cyanobacterial species were found to contribute substantially to the phytoplankton community (Supporting Information Table S4). These species apparently did not produce the specific PLFA C18:3 ω 6.

Data analyses

$\text{CO}_{2(\text{aq})}$ and $p\text{CO}_2$ were calculated from DIC concentrations, pH and water temperatures. The isotopic composition of $\text{CO}_{2(\text{aq})}$ was calculated from $\delta^{13}\text{C}_{\text{DIC}}$ with a correction for temperature (Mook et al. 1974). Isotope discrimination, or fractionation (ϵ), between phytoplankton and the carbon source $\text{CO}_{2(\text{aq})}$ was calculated as:

$$\epsilon_{\text{CO}_2-\text{phyto}} = \frac{\delta^{13}\text{C}_{\text{CO}_2} - \delta^{13}\text{C}_{\text{phyto}}}{1 + \delta^{13}\text{C}_{\text{phyto}}/1000} \quad (1)$$

Where phyto can mean either phytoplankton PLFA (for $\epsilon_{\text{CO}_2\text{-PLFA}}$) or phytoplankton biomass (for $\epsilon_{\text{CO}_2\text{-phyto}}$). Carbon isotopic composition of biomass was derived from the $\delta^{13}\text{C}$ of PLFAs by correcting for the isotopic offset between PLFAs and total cells. We used a correction of $+7.1 \pm 0.9\%$ for eukaryotic phytoplankton, $+4.1 \pm 0.8\%$ for diatoms, $+11.4 \pm 0.7\%$ for cyanobacteria, and $+2.2 \pm 0.1\%$ for bacteria (Taipale et al. 2015). Although depletion of lipid carbon isotopic composition with respect to biomass can vary widely (Schouten et al. 1998; Hayes 2001; Pel et al. 2004), the correction factors applied here were derived specifically for ω 3-PUFAs for phytoplankton and branched PLFAs for bacteria (Taipale et al. 2015) and are the best estimate we can use. However, we do realize that uncertainty in the applied correction factors is also reflected in the calculated $\delta^{13}\text{C}$ of biomass and small differences between $\delta^{13}\text{C}$ values of carbon pools and different producers/consumers should not be overinterpreted.

Concentrations of detritus (dead POC) were derived from POC by subtracting values for phytoplankton and bacteria (living POC):

$$C_{\text{det}} = C_{\text{POC}} - C_{\text{phyto}} - C_{\text{bact}} \quad (2)$$

Where C_{phyto} is calculated by multiplying the concentration of Chl *a* by 44 ± 17 (Montagnes et al. 1994) and C_{bact} is calculated using a ratio of C to FA of 50 (Middelburg et al. 2000). We assumed $\pm 20\%$ variation in the ratio of C to FA of 50 for bacteria. Since concentrations of terrestrial-derived long-chain saturated fatty acids (C20:0, C22:0, C24:0, C26:0) were too low to allow for reliable stable carbon isotope analyses, we calculated the carbon isotopic composition of detritus by mass balancing. Uncertainties in derived or composite variables such as $\delta^{13}\text{C}$ of phytoplankton, bacteria or detrital pools were calculated using error propagation techniques and uncertainties in measured $\delta^{13}\text{C}$ data, isotope fractionation factors and biomasses of phytoplankton and bacteria. A simple two-end

member isotope mixing model was used to calculate the dependence of bacteria on DOC, our proxy for allochthonous carbon resources.

Results

Sampling year vs. long-term averages

Temperature

Due to their close proximity, water temperatures showed little variation between sampling locations GM and BB, hence only temperatures from location GM are shown in Fig. 2a (black diamonds), with average temperatures over the period 2003–2014 shown as bars. In general, monthly water temperatures during the sampling campaign corresponded well with long-term averages. The average summer temperature of 2013 was warmer than the long-term average with temperatures of 21.1°C and 20.2°C, respectively, due to a warm August. During the winter of 2013–2014, the average temperature of 5.6°C was also somewhat warmer than the decadal average of 4.8°C. Conversely, the summer of 2014 was slightly colder than the long-term mean with an average temperature of 19.9°C. Both the sampling year and the long-term trend show that lowest temperatures were reached in December to February and spring warming started in March.

Chl *a*

Concentrations of Chl *a* at location GM during the sampling campaign fell within the range of natural variability (standard deviations of the long-term averages) (Fig. 2b). Chl *a* concentrations were relatively stable throughout the year, between 6 $\mu\text{g L}^{-1}$ and 17 $\mu\text{g L}^{-1}$ during most months. Highest concentrations, between 26 $\mu\text{g L}^{-1}$ and 31 $\mu\text{g L}^{-1}$, were measured from January to March. At location BB, Chl *a* concentrations also matched well with the long-term averages but showed a different seasonal trend compared to location GM (Fig. 2c), with two maxima observed each year (a smaller maximum in February and a more pronounced maximum in August–September). Chl *a* concentrations at BB were much higher than at GM, generally between 14 $\mu\text{g L}^{-1}$ and 31 $\mu\text{g L}^{-1}$ during our sampling year, with a maximum concentration of 87 $\mu\text{g L}^{-1}$ observed in September 2013. The February maximum was lower with a concentration of 61 $\mu\text{g L}^{-1}$. In 2014, there was no clear maximum observed in August/September.

pH

At sampling location GM, pH values measured during our sampling campaign did not consistently correspond to the long-term averages (Fig. 2d). During the last decade, average pH values generally varied between 8.0 and 8.3, with higher pH values of 8.6 and 8.9 in June and July. However, during the 2013–2014 sampling year, pH values were around 7.5 in September, November, and December, which were lower than during any other year of the 2003–2014 period and clearly deviated from the trend. In 2014, pH values in August and September were higher than usual, around 9.2. It

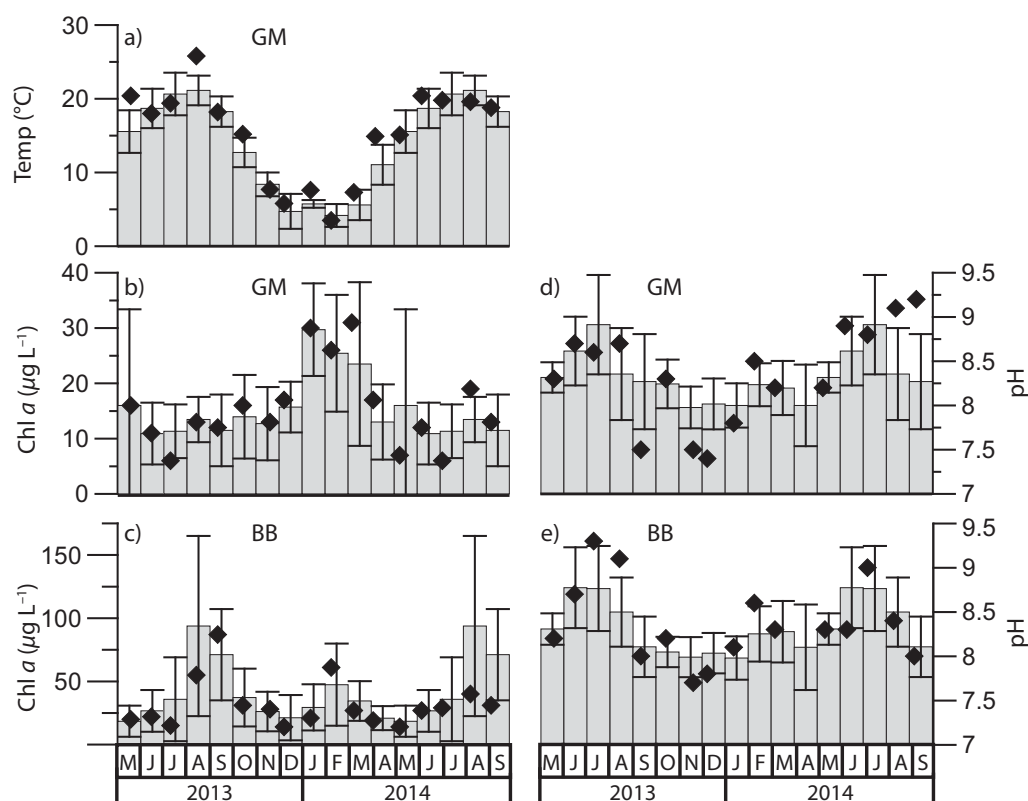


Fig. 2. (a) Water temperatures ($^{\circ}\text{C}$), concentrations of Chl *a* ($\mu\text{g L}^{-1}$) at sites (b) GM and (c) BB, and pH values at sites (d) GM and (e) BB. Values as measured during the 2013–2014 sampling campaign are shown as black diamonds. Gray-shaded bars represent long-term averages (with error bars) for data measured between 2003 and 2014.

is notoriously difficult to do correct pH analyses on an absolute scale hence we also looked at bicarbonate concentrations (data not shown), which showed comparable values for our time series compared to the long-term averages. However, these values could not be used to calculate pH since reliability of alkalinity analyses, and hence bicarbonate concentrations, tends to be reduced in lake water due to the buffering capacity of humic substances near the endpoint of alkalinity titrations (Wilson 1979). At the moment, we cannot explain the aberrant pH values compared to the long-term trend since other parameters matched well. Since we cannot fully exclude analytical errors as a cause for these deviations, we used long-term averages of pH values in our calculations of $\text{CO}_{2(\text{aq})}$ and $p\text{CO}_2$. At site BB, the long-term averages were very similar to site GM, ranging between 8.0 and 8.3 with an average annual maximum of 8.5–8.8 from June–August (Fig. 2e). At this site, pH values during the 2013–2014 sampling period corresponded well with the long-term averages.

$\delta^{13}\text{C}$ of inorganic carbon pools

DIC

At sampling site GM, concentrations of DIC showed considerable variability throughout the year (Fig. 3a, left) with

maximum concentrations around 2.0 mmol L^{-1} in late spring/early summer (May, June) and minimum concentrations in late summer (August, September) around 1.2 mmol L^{-1} and 0.85 mmol L^{-1} in 2013 and 2014, respectively. Stable carbon isotopes of DIC at site GM showed highest (more enriched) $\delta^{13}\text{C}$ values between -0.9‰ and -0.6‰ in June and July and lowest (most depleted) values between -4.6‰ and -3.8‰ during winter months November–January (Fig. 3b, left, Supporting Information Table S2).

DIC concentrations at sampling site BB showed a similar trend as site GM, but the maximum concentrations were higher, resulting in a larger annual range (Fig. 3a, right). Minimum concentrations of 1.5 mmol L^{-1} and 1.3 mmol L^{-1} were observed in July 2013 and 2014. During other months, DIC concentrations were relatively stable between 2.0 mmol L^{-1} and 2.5 mmol L^{-1} , with the exception of May 2013 when a peak concentration of 2.8 mmol L^{-1} was observed. Carbon isotope values of DIC at site BB (Fig. 3b, right, Supporting Information Table S2) were substantially lower than at site GM, with $\delta^{13}\text{C}$ values ranging between -9.5‰ and -3.8‰ . Most depleted $\delta^{13}\text{C}$ values were observed in July, and November to January. The depleted $\delta^{13}\text{C}$ value in July 2013 deviated substantially from the generally more enriched values during other summer months. During this

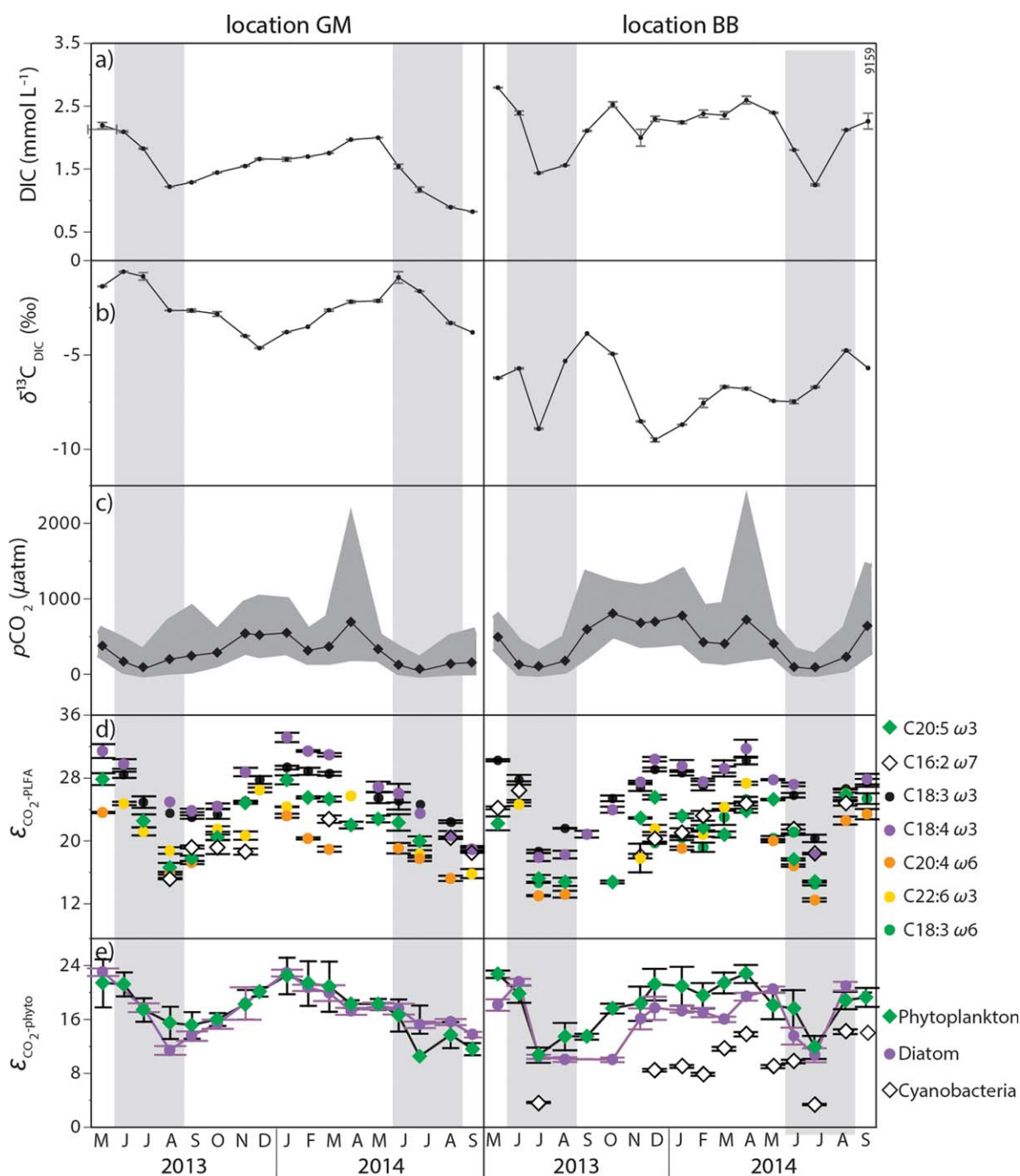


Fig. 3. (a) DIC concentrations (mmol C L^{-1}) and (b) DIC carbon isotopic compositions (‰ vs. V-PDB), (c) average $p\text{CO}_2$ concentrations (μatm) with gray envelopes mean \pm standard deviations as derived from pH values, (d) fractionation values (ϵ , in ‰ vs. V-PDB) of individual PLFAs relative to $\text{CO}_{2(\text{aq})}$ as calculated from $\delta^{13}\text{C}_{\text{DIC}}$ at location GM (left) and BB (right). Carbon isotopic compositions of individual PLFAs were not corrected for isotopic offset between PLFA and total cells. (e) Fractionation values (‰ vs. V-PDB) between $\text{CO}_{2(\text{aq})}$ and weighted averages of phytoplankton, diatom, and cyanobacterial $\delta^{13}\text{C}$ after correction for the isotopic offset between PLFA and total cells. Location GM is shown left and BB is shown right. Gray shaded areas correspond to summer months: June–August.

month, the observed combination of a high pH (Fig. 2e) and low $p\text{CO}_2$ (Fig. 3c) may have caused chemically enhanced diffusion (CED). During CED, a major source of DIC in water

is the reaction between atmospheric CO_2 and OH^- , instead of the more general reaction between CO_2 and H_2O . The latter reaction results in a fractionation of $+8\text{‰}$, compared to a

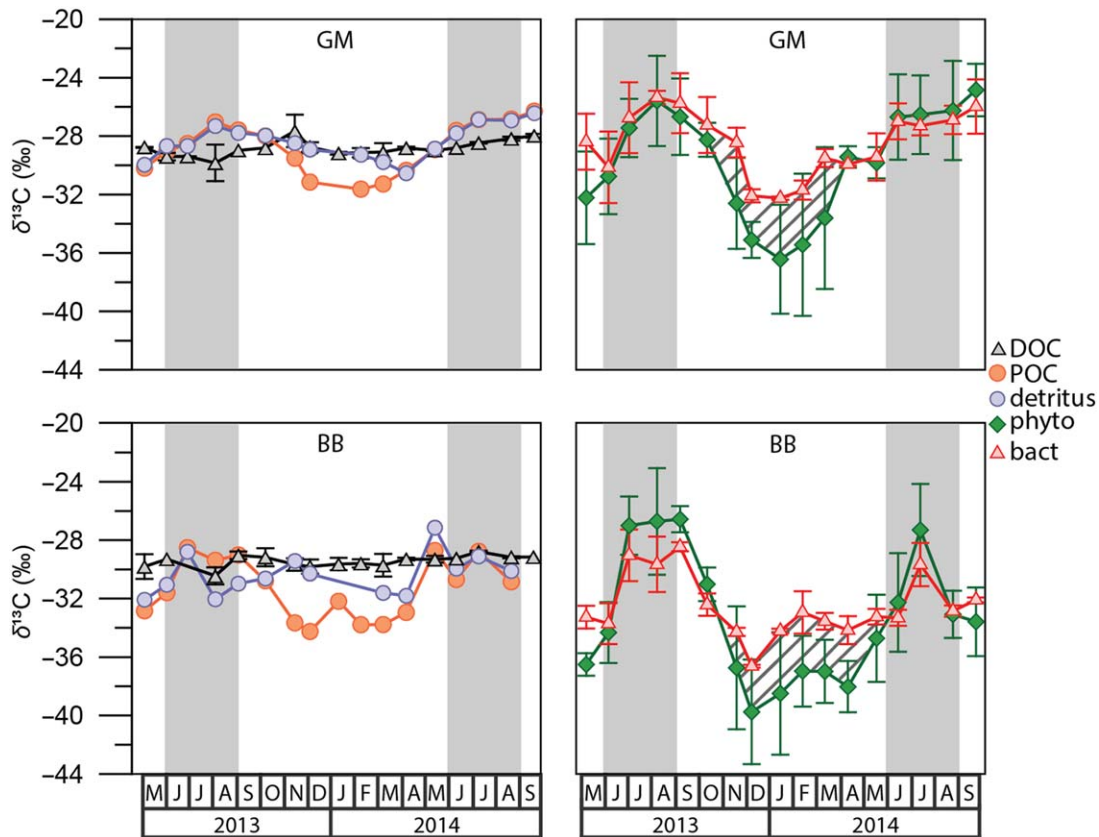


Fig. 4. Left: Seasonal variations in carbon isotopic composition ($\delta^{13}\text{C}$ in ‰ vs. V-PDB \pm SD where possible) of carbon pools DOC (black), POC (orange), and detritus (purple). An outlier in $\delta^{13}\text{C}_{\text{det}}$ in February 2014 at site BB (-9.4‰) is not plotted as it is strongly influenced by exceptionally high Chl *a* concentrations. Right: Seasonal variations in carbon isotopic composition ($\delta^{13}\text{C}$ in ‰ vs. V-PDB \pm SD) of bacterial biomass (red) and phytoplankton biomass (green). The gray hatched areas represent offset of $\delta^{13}\text{C}_{\text{bact}}$ from $\delta^{13}\text{C}_{\text{phyto}}$, likely as a result of enhanced contribution of DOC (allochthonous carbon) to bacterial biomass. Values for site GM are shown at the top, site BB is plotted at the bottom. Gray shaded areas correspond to summer months: June–August. Data with uncertainty are presented in Supporting Information Table S2.

fractionation of -15‰ during CED, which hence results in a more depleted $\delta^{13}\text{C}$ of DIC (Bade and Cole 2006; Bontes et al. 2006). This may thus explain the observed more negative values in July 2013. Overall, most enriched values were observed in August and September of both sampling years.

$p\text{CO}_2$

At sampling site GM, the calculated $p\text{CO}_2$ values were relatively low, between minima of $67 \mu\text{atm}$ and $43 \mu\text{atm}$ in July 2013 and 2014, respectively, to maxima around $540 \mu\text{atm}$ in the winter of 2013–2014 and $670 \mu\text{atm}$ in April 2014 (Fig. 3c, left). Variability in $p\text{CO}_2$ values at site BB was similar, with minimum values around $79 \mu\text{atm}$ and $69 \mu\text{atm}$ in July 2013 and 2014, respectively, and a maximum around $800 \mu\text{atm}$ in October 2013 (Fig. 3c, right). Given the relatively high standard deviations on the calculated $p\text{CO}_2$ values (Fig. 3c, grey envelopes), we will refrain from discussing the numbers in detail. Still these numbers indicate very low contributions of CO_2 to the total DIC pool, hence $\delta^{13}\text{C}_{\text{CO}_2}$ will not be biased by uncertainties in $p\text{CO}_2$ values.

$\delta^{13}\text{C}$ of biomass and organic carbon pools

Weighted averages of $\delta^{13}\text{C}$ values of bacterial biomass were relatively enriched in $\delta^{13}\text{C}$ during summer and relatively depleted in $\delta^{13}\text{C}$ during winter (Fig. 4, Supporting Information Table S1). At site GM, $\delta^{13}\text{C}_{\text{bact}}$ showed an annual range of 6.9‰ varying between $-32.3 \pm 0.1\text{‰}$ and $-25.4 \pm 0.5\text{‰}$. At site BB, $\delta^{13}\text{C}_{\text{bact}}$ values had a higher annual span of 8.1‰ , and showed more depleted $\delta^{13}\text{C}_{\text{bact}}$ ranging between $-36.6 \pm 0.1\text{‰}$ and $-28.5 \pm 0.3\text{‰}$.

Weighted averages of $\delta^{13}\text{C}$ values of phytoplankton biomass showed comparable seasonal changes as $\delta^{13}\text{C}_{\text{bact}}$ with enriched values during summer and depleted values during winter (Fig. 4, green). However, the annual range was larger than observed for bacteria. At site GM, $\delta^{13}\text{C}_{\text{phyto}}$ values had an annual span of 11.6‰ , ranging between $-36.4 \pm 3.7\text{‰}$ and $-24.8 \pm 1.8\text{‰}$. At site BB, $\delta^{13}\text{C}_{\text{phyto}}$ values had a somewhat higher annual span of 13.2‰ , and showed more depleted $\delta^{13}\text{C}_{\text{phyto}}$ ranging between $-39.8 \pm 3.6\text{‰}$ and $-26.6 \pm 0.9\text{‰}$.

POC also showed clear seasonal differences at both sampling sites (Fig. 4, orange, Supporting Information Table S2).

Table 1. Average $\delta^{13}\text{C}$ values (in ‰ vs. V-PDB \pm SD; $n = 2$) of terrestrial and aquatic vegetation from Lake Naarden during fall 2015.

Vegetation		$\delta^{13}\text{C}$ (‰)
Terrestrial	Hair moss (<i>Polytrichaceae</i>)	-29.1 ± 0.1
Terrestrial	Reed leaf (<i>P. australis</i>)	-26.9 ± 0.1
Terrestrial	Reed stem (<i>P. australis</i>)	-26.6 ± 0.4
Terrestrial	Marsh fern (<i>T. palustris</i>)	-29.3 ± 0.1
Aquatic	Water lily (<i>Nymphaeaceae</i>)	-25.5 ± 0.1
Aquatic	Common stonewort (<i>Characeae</i>)	-16.4 ± 0.5
Aquatic	Shining pontweed (<i>P. lucens</i>)	-27.8 ± 0.4

Lowest, most depleted $\delta^{13}\text{C}$ values were observed during winter and early spring (November to April) with values around -31.6‰ at site GM and -34.4‰ at site BB. From April onward, $\delta^{13}\text{C}_{\text{POC}}$ increased until maxima were reached from July to September, with values around -26.3‰ at site GM and -28.5‰ at site BB. The annual range of $\delta^{13}\text{C}_{\text{POC}}$ values was 5.3‰ at site GM and 5.7‰ at site BB. At both sampling sites, detritus was the dominant component of the POC pool (Supporting Information Table S3). At site GM, $77\% \pm 8\%$ to $92\% \pm 3\%$ of POC consisted of detritus from April to October. During winter months (November to March), detritus contributed a smaller fraction of POC, between $52\% \pm 17\%$ and $71\% \pm 10\%$, indicating highest living biomass contributions during winter, as already shown by the Chl *a* data (Fig. 2b). Calculated stable carbon isotopic compositions of detritus at site GM varied between $-26.4 \pm 1.5\text{‰}$ and $-30.5 \pm 3.5\text{‰}$ (Fig. 4, Supporting Information Table S2). At site BB, the relative contributions of detritus and living biomass to the POC pool showed more variability. During summer months (from April to July in 2013 and until September in 2014), $69\% \pm 11\%$ to $83\% \pm 6\%$ of POC was detritus. From August 2013 to March 2014, the fraction of detritus was much lower, ranging between $40\% \pm 22\%$ and $80\% \pm 7\%$, with the exception of February 2014. In this month, an exceptionally large contribution of phytoplankton biomass to POC was derived from Chl *a* data and hence a low contribution resulted for detritus of $\sim 2\% \pm 36\%$ of the POC pool. At site BB, calculated $\delta^{13}\text{C}_{\text{det}}$ varied between $-27.1 \pm 4.2\text{‰}$ and $-32.1 \pm 4.1\text{‰}$ (Fig. 4), except for February 2014 during which the calculation was strongly influenced by the unusually high Chl *a* concentrations. Stable carbon isotopic compositions of DOC were stable throughout the year with $\delta^{13}\text{C}$ values of $-28.8 \pm 0.6\text{‰}$ for GM and $-29.5 \pm 0.4\text{‰}$ for BB (Fig. 4, black, Supporting Information Table S2).

Carbon isotopic compositions of abundant species of littoral and terrestrial macrophytes (Table 1) were typical for vegetation using the C3 photosynthetic pathway with $\delta^{13}\text{C}$ values of $-29.1 \pm 0.1\text{‰}$ for *Polytrichaceae* (hair moss), $-26.9 \pm 0.1\text{‰}$ and $-26.6 \pm 0.4\text{‰}$ for *Phragmites australis*

(reed) leaf and stem, respectively, and $-29.3 \pm 0.1\text{‰}$ for *Thelypteris palustris* (marsh fern). Aquatic vegetation had $\delta^{13}\text{C}$ values of $-25.5 \pm 0.1\text{‰}$ for *Nymphaeaceae* (water lily), $-27.8 \pm 0.4\text{‰}$ for *Potamogeton lucens* (shining pontweed), and markedly different $\delta^{13}\text{C}$ value of $-16.4 \pm 0.5\text{‰}$ for *Characeae* (common stonewort) (Table 1). A potential contamination with CaCO_3 was specifically excluded using multiple decalcification steps.

Bacterial dependence on allochthonous organic carbon was calculated from a standard one-isotope-two-sources isotope mixing model using the $\delta^{13}\text{C}$ of DOC as proxy for terrestrial organic matter and the $\delta^{13}\text{C}$ of phytoplankton as representative of locally produced organic matter. Bacterial dependence on DOC varied between 39% and 77% at site GM and between 17% and 64% in basin BB. This dependence could only be calculated during winter and spring months because of overlapping $\delta^{13}\text{C}$ values during summer (Fig. 4).

Phytoplankton fractionation

Fractionation values between phytoplankton PLFAs and the carbon source $\text{CO}_{2(\text{aq})}$ ($\epsilon_{\text{CO}_2\text{-PLFA}}$) are shown in Fig. 3d (GM left, BB right) and show substantial differences in $\epsilon_{\text{CO}_2\text{-PLFA}}$ between individual PLFAs, with the seasonal changes being similar and in phase for the different PLFAs. At both sites, lowest fractionation values were observed at the end of summer and highest fractionation was observed during winter. Although $\delta^{13}\text{C}_{\text{DIC}}$ differed appreciably between the two basins, individual phytoplankton PLFAs displayed similar ϵ values at both sites, with highest fractionation values for PLFAs C18:3 ω 3 and C18:4 ω 3, ranging between $18.9 \pm 0.2\text{‰}$ and $29.3 \pm 0.2\text{‰}$ for C18:3 ω 3 and between $19.0 \pm 0.3\text{‰}$ and $33.2 \pm 0.6\text{‰}$ for C18:4 ω 3 at site GM. At site BB, ϵ values were similar, ranging between $18.7 \pm 0.2\text{‰}$ and $30.3 \pm 0.1\text{‰}$ for PLFA C18:3 ω 3 and between $17.9 \pm 0.5\text{‰}$ and $31.7 \pm 1.1\text{‰}$ for PLFA C18:4 ω 3. Lowest ϵ values at site GM were observed in PLFAs C20:4 ω 6 and C16:2 ω 7, ranging between $15.2 \pm 0.3\text{‰}$ and $23.6 \pm 0.1\text{‰}$ and between $15.2 \pm 0.1\text{‰}$ and $22.8 \pm 0.5\text{‰}$, respectively. At site BB, lowest ϵ values were found for PLFA C20:4 ω 6, ranging between $12.5 \pm 0.2\text{‰}$ and $23.4 \pm 0.7\text{‰}$, and for PLFA C20:5 ω 3, ranging between $14.8 \pm 0.2\text{‰}$ and $25.9 \pm 0.7\text{‰}$. Additionally, cyanobacterial PLFA C18:3 ω 6 at location BB also showed relatively low ϵ values, ranging between $14.5 \pm 0.2\text{‰}$ and $25.6 \pm 0.6\text{‰}$.

Stable carbon isotopic fractionation between $\text{CO}_{2(\text{aq})}$ and PLFA-based phytoplankton biomass ($\epsilon_{\text{CO}_2\text{-phyto}}$) are shown in Fig. 3e. Since the isotopic offset between PLFA and total cells is different for diatoms compared to other phytoplankton species (Taipale et al. 2015), the resulting $\epsilon_{\text{CO}_2\text{-phyto}}$ were plotted separately (Fig. 3e). At sampling site GM, there was little difference between $\epsilon_{\text{CO}_2\text{-phyto}}$ of diatoms compared to other eukaryotic phytoplankton (Fig. 3e, left), with minimum values of $11.9 \pm 0.7\text{‰}$ and $15.1 \pm 2.0\text{‰}$, respectively, in 2013 and around $14.2 \pm 0.4\text{‰}$ and $11.5 \pm 0.9\text{‰}$, respectively,

in 2014. Maximum $\epsilon_{\text{CO}_2\text{-phyto}}$ values during winter were around $23.5 \pm 0.6\text{‰}$ for both diatoms and other eukaryotic phytoplankton species. At site BB, the difference in $\epsilon_{\text{CO}_2\text{-phyto}}$ between eukaryotic phytoplankton and diatoms was more apparent, with generally lower ϵ values for diatoms (Fig. 3e, right). Minimum $\epsilon_{\text{CO}_2\text{-phyto}}$ of eukaryotic phytoplankton was $10.7 \pm 1.1\text{‰}$ and $11.8 \pm 1.7\text{‰}$ in July 2013 and 2014, respectively, with maximum fractionation values between $19.5 \pm 1.9\text{‰}$ and $22.7 \pm 1.3\text{‰}$ from December 2013 to April 2014. Diatom fractionation decreased to around $10.5 \pm 0.3\text{‰}$ from June to October 2013 and was stable around 17‰ during winter and early spring (November to March), reaching a maximum ϵ value of $22.0 \pm 0.5\text{‰}$ in June 2013. A minimum fractionation of $10.5 \pm 0.3\text{‰}$ was observed in August 2013. Substantially lower $\epsilon_{\text{CO}_2\text{-phyto}}$ values were observed for PLFA-based cyanobacterial biomass, with minimum values of $2.9 \pm 0.1\text{‰}$ and $2.7 \pm 0.1\text{‰}$ in July 2013 and 2014, respectively, and a maximum fractionation of $13.2 \pm 0.3\text{‰}$ and $13.6 \pm 0.3\text{‰}$ observed in April 2014 and August 2014, respectively.

Discussion

Time series

Chl *a* concentrations, representing phytoplankton biomass, varied considerably between locations GM (Fig. 2b) and BB (Fig. 2c). At site GM, Chl *a* concentrations peak from January to March, but it is likely that absolute production is higher during spring (and fall) blooms but this is likely compensated by higher grazing pressures at the same time. At site BB, Chl *a* concentrations, or production which escapes grazing (i.e., net production), is highest during late summer (August, September), with a smaller peak in February (Fig. 2c). It seems that net production in BB is higher and more prone to bloom formation compared to GM.

The 17-month sampling period covered two summers and a winter, thereby capturing the full range of seasonal variability in terms of temperatures and light. Overall, variability during the sampling period from May 2013 to September 2014 is in line with that observed over a longer timescale in terms of temperatures, phytoplankton biomass, and inorganic carbon chemistry (Fig. 2). We therefore believe that the obtained results can be interpreted as representing common conditions. Also the sampling interval used seems to nicely capture the lake's variability over the year, based on the observed gradual changes in the time series.

DIC concentrations and $\delta^{13}\text{C}$

In most lakes, DIC concentrations generally vary between $0.1 \text{ mmol C L}^{-1}$ and 1 mmol C L^{-1} but the naturally occurring range is much larger ($<0.02 \text{ mM}$ to $>5 \text{ mM}$) and concentrations within systems can be highly variable (Cole and Prairie 2009). At site GM, DIC concentrations show a large range, varying from around $1.3 \text{ mmol C L}^{-1}$ during summer to $\sim 2.7 \text{ mmol C L}^{-1}$ during spring (Fig. 3a, left). DIC

concentrations at site BB were higher during most months and were rather stable around $2.3 \text{ mmol C L}^{-1}$ from October to March. DIC isotopic compositions at site GM (Fig. 3b, left) and BB (Fig. 3b, right) showed different values and seasonality with $\delta^{13}\text{C}_{\text{DIC}}$ values 2–7‰ lower at site BB compared to site GM. These lower values can be due to higher respiration at this more eutrophic site and/or input of small amounts of a relatively depleted source of inorganic carbon (e.g., methane, $\delta^{13}\text{C}$ around -60‰) adding to the DIC pool in basin BB. Enhanced respiration would also explain the somewhat higher DIC concentrations, but some contribution of groundwater-derived methane to the DIC pool at site BB cannot be ruled out, since there is groundwater seeping into this basin (P. Schot pers. comm.).

Both DIC concentrations and $\delta^{13}\text{C}_{\text{DIC}}$ are affected by production and respiration, with primary production resulting in lower DIC concentrations and enriched $\delta^{13}\text{C}_{\text{DIC}}$ due to isotopic fractionation by phytoplankton: the preferential uptake of ^{12}C over ^{13}C during photosynthesis. Conversely, respiration releases relatively light carbon thereby increasing concentrations and lowering $\delta^{13}\text{C}_{\text{DIC}}$. From January until summer, the balance between production and respiration shifts and causes increasing $\delta^{13}\text{C}_{\text{DIC}}$ at both sites (Fig. 3b). During and after summer, the opposite occurs, when $\delta^{13}\text{C}_{\text{DIC}}$ values decrease. Concentrations of aqueous dissolved CO_2 ($p\text{CO}_{2(\text{aq})}$) as derived from (DIC), pH and water temperatures are lower at sampling site GM, compared to site BB during most of the year (Fig. 3c). As expected, $p\text{CO}_2$ concentrations decrease to very low values during periods of intense primary production (June–August), while $p\text{CO}_2$ maxima are observed during winter months when respiration rates are relatively high. The calculated $p\text{CO}_2$ trends correspond well with variability in $\delta^{13}\text{C}_{\text{DIC}}$, with minima in $p\text{CO}_2$ corresponding to more enriched $\delta^{13}\text{C}_{\text{DIC}}$ and maxima in $p\text{CO}_2$ co-occurring with more depleted $\delta^{13}\text{C}_{\text{DIC}}$. Only in July 2013 in basin BB, when chemical enhanced diffusion might have been important (see above), lower $p\text{CO}_2$ does not correspond to enriched $\delta^{13}\text{C}_{\text{DIC}}$.

Phytoplankton $\delta^{13}\text{C}$ and fractionation

The stable carbon isotopic composition of PLFAs did not only vary clearly throughout the year, but $\delta^{13}\text{C}$ values of individual PLFAs were also different by up to 11.3‰ and 10.1‰ at locations GM and BB, respectively, within the same month (Supporting Information Table S1). This variation in $\delta^{13}\text{C}$ of individual PLFAs may partly result from species-specific isotopic offsets between lipids and total cells. The magnitude of this offset is not well constrained and the applied correction for this offset can be highly variable (Schouten et al. 1998; Pel et al. 2004; Taipale et al. 2015). Additionally, the $\delta^{13}\text{C}$ of phytoplankton biomass can be influenced by several species-specific factors resulting in species-specific isotopic discrimination (or fractionation, ϵ) between carbon source ($\text{CO}_{2(\text{aq})}$) and consumers. For example, differences in cell size and permeability (CO_2

diffusion into or leakage out of cells) (Popp et al. 1998), the enzymatic pathway used during photosynthesis, the kinetics of carbon uptake (active vs. diffusion), and the uptake of different carbon species (see below) all result in different ϵ values for different species (Peterson and Fry 1987; O'Leary 1988; Farquhar et al. 1989; Laws et al. 1995). The PLFAs found in Lake Naarden have different ϵ values relative to $\text{CO}_{2(\text{aq})}$ (Fig. 3d), which likely reflects variability in their respective source organisms or the relative uptake of different carbon species.

Although the observed PLFAs may have been produced by several source organisms at the same time, the observed suite of PLFAs allows us to distinguish between, and to calculate, $\delta^{13}\text{C}$ (weighted averages) of diatoms compared to other eukaryotic phytoplankton and cyanobacteria (the latter at site BB only) (Fig. 3e). Differences in fractionation between $\text{CO}_{2(\text{aq})}$ and eukaryotic phytoplankton and between $\text{CO}_{2(\text{aq})}$ and diatoms are small. The range in ϵ values found here for diatoms and other eukaryotic phytoplankton ($10.5 \pm 0.3\text{‰}$ to $23.5 \pm 0.6\text{‰}$) corresponds well with values found in other studies, e.g., 7–18‰ under different light conditions (Rost et al. 2002), 7–27‰ in a tidal freshwater estuary (Van den Meersche et al. 2009), 8–25‰ in lakes along a trophic gradient (De Kluijver et al. 2014), 7–33‰ in a biomanipulation study (Bontes et al. 2006), and other studies (Brett 2014). The observed ϵ values of cyanobacteria at site BB are substantially lower than ϵ values for both diatoms and eukaryotic phytoplankton in general, likely related to morphological and physiological differences in, e.g., cell walls, and the combination of photosynthesis and respiration within the same compartment (Vermaas 2001), and the presence of carboxyzomes (microstructures involved in increasing Rubisco efficiency) in cyanobacteria. Observed fractionation values for cyanobacterial biomass are in line with an average ϵ value of 12.2‰ reported by Bontes et al. (2006).

The relative uptake of CO_2 and bicarbonate affects photoautotrophs fractionation values not only between species, but also throughout the year. This is a result of the $\sim 10\text{‰}$ isotopic fractionation during the conversion of $\text{CO}_{2(\text{g})}$ to HCO_3^- (Mook et al. 1974). Rubisco requires CO_2 , which can be limiting in lacustrine environments, e.g., during periods (or at depths) of high productivity, while HCO_3^- is abundant. To keep up photosynthesis during periods of low ($\text{CO}_{2(\text{aq})}$), aquatic photosynthesizers have developed carbon concentrating mechanisms (Lucas and Berry 1985), e.g., using carbonic anhydrase (CA), a family of enzymes that catalyses interconversion between CO_2 and bicarbonate. A relationship between fractionation values and concentrations of $\text{CO}_{2(\text{aq})}$ would thus be expected, with higher ϵ when $p\text{CO}_{2(\text{aq})}$ is higher. This relationship has been confirmed in several studies, which have shown the response of ϵ to changing $p\text{CO}_{2(\text{aq})}$ to be species-specific (Degens et al. 1968; Mizutani and Wada 1982; Finlay 2004; Hoins et al. 2015). At both sampling sites in Lake Naarden, a general seasonal trend of higher $p\text{CO}_{2(\text{aq})}$ occurring with higher $\epsilon_{\text{CO}_2\text{-phyto}}$

Table 2. Pearson correlations between $\epsilon_{\text{CO}_2\text{-phyto/diatom/cyano}}$ and $p\text{CO}_2$ at both sampling sites, where n.d. means not detected. R values for diatoms and cyanobacteria were not statistically significant due to low R value (diatoms) or low n (cyanobacteria).

	Location GM	Location BB
$\epsilon_{\text{CO}_2\text{-phyto}}$	$R=0.518$ ($p<0.05$)	$R=0.415$ ($p<0.10$)
$\epsilon_{\text{CO}_2\text{-diatom}}$	$R=0.491$ ($p<0.10$)	$R=0.265$
$\epsilon_{\text{CO}_2\text{-cyano}}$	n.d.	$R=0.423$

(Fig. 3c,e) is observed. Calculated Pearson correlations however, showed only weak to moderate positive correlations at site GM and no to weak positive correlations at site BB (Table 2). This probably reflects phytoplankton isotopic discrimination depending on many other factors as well such as DIC concentrations (Taipale et al. 2016b), or growth rates (μ), with higher growth rates resulting in lower ϵ values. Correspondingly, other studies observed stronger correlations between ϵ values and $\mu/(\text{CO}_{2(\text{aq})})$ (Laws et al. 1995; Popp et al. 1998; Keller and Morel 1999; Bontes et al. 2006; Van Breugel et al. 2006). Additionally, irradiance and light cycles have also been shown to have a major influence on $\epsilon_{\text{CO}_2\text{-phyto}}$, stronger even than $p\text{CO}_{2(\text{aq})}$ and growth rates (Burkhardt et al. 1999; Rost et al. 2002). As copious factors influence $\epsilon_{\text{CO}_2\text{-phyto}}$ and a large variety in correlations has been observed (positive and negative, linear and nonlinear), it is practically impossible to determine which factors exactly contributed to the annual variability we observed in the natural system studied here. Nevertheless, a trend can be observed of highest ϵ at times when $p\text{CO}_2$ is also highest (Fig. 3) during periods of typically low production rates. Additionally, ϵ values decrease during spring and summer when $p\text{CO}_2$ decreases and production rates are typically enhanced. This trend is suggestive of uptake of bicarbonate as an alternative carbon source during periods when the concentration of $\text{CO}_{2(\text{aq})}$ is low (Hoins et al. 2016).

POC

POC contains living biomass of phytoplankton and bacteria as well as dead organic matter (detritus) from these and other organisms, but it can also contain allochthonous organic carbon, such as small pieces of terrestrial vegetation. At site GM, seasonal changes in the carbon isotopic composition of POC are similar to the seasonality observed in the $\delta^{13}\text{C}$ of bacterial and phytoplankton biomass (Fig. 4). Allochthonous detritus with invariable $\delta^{13}\text{C}$ around -27‰ to -29‰ (Table 1) dominates the concentration (Supporting Information Table S3) and the $\delta^{13}\text{C}$ composition of total POC pool. The moderate seasonal fluctuation in $\delta^{13}\text{C}$ in total POC is likely caused by the more pronounced fluctuation in algal POC that contribute from 5% to 36% to total POC (Supporting Information Table S3). At site BB, $\delta^{13}\text{C}_{\text{bact}}$ and

$\delta^{13}\text{C}_{\text{POC}}$ are similar during most months, but the amplitude of variation in $\delta^{13}\text{C}_{\text{phyto}}$ is higher, showing more enriched values during summer and more depleted values during winter (Fig. 4), which is in line with living biomass making up a relatively larger part of the POC pool in BB compared to site GM (Supporting Information Table S3). Overall, the isotopic composition of the POC pools at BB and GM differ considerably, but both consist mostly of detritus throughout the year.

Carbon isotopic compositions of terrestrial and aquatic vegetation from Lake Naarden between -25.5% and -29.3% are typical for vegetation using the C3 photosynthetic pathway, with aquatic vegetation showing somewhat more enriched $\delta^{13}\text{C}$ compared to terrestrial vegetation (Table 1). Only *Characeae*, or common stonewort having C3 and C4 pathways (Feeley 1999), has a substantially more enriched $\delta^{13}\text{C}$ of -16.4% despite careful decalcification steps during sample preparation. In general, $\delta^{13}\text{C}$ values of POC are lower than $\delta^{13}\text{C}$ values of the aquatic and terrestrial vegetation (Fig. 4). Both terrestrial and aquatic vegetation sources likely contribute to the POC pool, stabilizing values, with the more negative values resulting from enhanced phytoplankton production.

Carbon subsidies to bacteria

Bacterial production can be sustained by locally produced fresh algal biomass, its detritus, macrophytes, and locally produced or allochthonous DOC. The seasonal trend observed in the isotopic composition of bacterial carbon ($\delta^{13}\text{C}_{\text{bact}}$) is similar to the trend observed in POC (Fig. 4) and phytoplankton biomass ($\delta^{13}\text{C}_{\text{phyto}}$, Fig. 4), albeit with a smaller amplitude than phytoplankton. Strong positive correlations are observed between $\delta^{13}\text{C}_{\text{phyto}}$ and $\delta^{13}\text{C}_{\text{bact}}$ at site GM ($R = 0.909$, $p < 10^{-5}$) and site BB ($R = 0.935$, $p < 10^{-5}$), indicating that the seasonal variation in $\delta^{13}\text{C}_{\text{bact}}$ derives mostly from variations in $\delta^{13}\text{C}$ of autochthonous, fresh organic matter. However, $\delta^{13}\text{C}_{\text{bact}}$ has an annual range of 6.9% and 8.1% at sites GM and BB, respectively, while this range is 11.6% and 13.2% for phytoplankton, indicative of contributions from another carbon source. Because the correlation between phytoplankton and bacterial $\delta^{13}\text{C}$ is strong but the effects of seasonal variability in $\delta^{13}\text{C}_{\text{phyto}}$ are dampened in bacteria, the supplementary carbon source must have a stable carbon isotopic signature.

Terrestrial vegetation using atmospheric carbon dioxide shows limited isotopic variability and bacterial utilization of terrestrial plants or DOC derived from terrestrial plants might explain the attenuated seasonality (Fig. 4). The DOC pool has a constant carbon isotopic composition throughout the year, with rather low values around $-28.8 \pm 0.6\%$ at site GM and $-29.5 \pm 0.4\%$ at site BB (Fig. 4). Stability of $\delta^{13}\text{C}_{\text{DOC}}$ throughout the year and uncoupling between the stable carbon isotopic compositions of DOC and POC has previously been observed and was attributed to rapid mineralization of

phytoplankton-derived DOC resulting in low contributions ($< 1\%$) of locally produced DOC to the total DOC pool (Morana et al. 2015). Similarly, in a productive system such as Lake Naarden, the stability of $\delta^{13}\text{C}_{\text{DOC}}$ likely also indicates that concentrations of locally produced phytoplankton-derived DOC are much lower than allochthonous DOC and hence too low to affect the isotopic signal of the large total DOC pool. Although likely very small, we cannot calculate the exact contribution of phytoplankton-produced DOC to the total DOC pool, hence we assume the DOC pool in Lake Naarden to consist of allochthonous carbon (hence representing DOC) and we use $\delta^{13}\text{C}_{\text{phyto}}$ to represent the autochthonous organic carbon source to bacteria. We realize that the DOC pool has a highly variable composition (Fry et al. 1998) and that there is likely variability in the $\delta^{13}\text{C}$ of the individual compounds making up the DOC. Since certain compounds will be preferentially consumed, the carbon isotopic composition of the DOC pool as a whole may be somewhat different from the actual food used from that pool by bacteria. Still, even terrestrially derived DOC, although traditionally assumed to be aged and refractory, has been shown to fuel at least parts of the food web (Battin et al. 2008; Cole et al. 2011) and here $\delta^{13}\text{C}_{\text{DOC}}$ represents the best approximation for allochthonous carbon.

During some months, carbon isotopic compositions of potential sources (phytoplankton, macrophytes, and DOC) and bacteria were very similar and thus could not be used to accurately calculate bacterial dependence on allochthonous carbon (Fig. 4). Still, it is clear that during most of the year, $\delta^{13}\text{C}_{\text{bact}}$ closely follows $\delta^{13}\text{C}_{\text{phyto}}$, especially at site GM (Fig. 4), suggesting that most bacterial carbon derives from phytoplankton (autochthonous) production. At site BB, bacterial biomass is depleted compared to phytoplankton by $1\text{--}2\%$ even during summer months that are characterized by high phytoplankton productivity, which may indicate that, in addition to phytoplankton, a more ^{13}C -depleted carbon source is used by bacteria. However, given the uncertainty in the applied correction for the isotopic offset between PLFA and total cells (section 2.4), this difference seems minor.

During winter and spring substantial differences were observed in $\delta^{13}\text{C}$ between bacterial biomass and phytoplankton biomass and DOC (Fig. 4). During these months, bacterial dependence on DOC varied between 39% and 77% at site GM and between 17% and 46% at site BB. These numbers are in line with previous studies (De Kluijver et al. 2015), in which also lower allochthonous contributions were observed in a more eutrophic lake (Cole et al. 2006), likely related to greater availability of phytoplankton carbon sources in eutrophic lakes (Taipale et al. 2016a). Both basins are eutrophic, have high DOC concentrations ($0.8\text{--}1.2 \text{ mmol C L}^{-1}$; Waternet database), and a relatively short water residence times (~ 2 months, Vink 2013). And DOC availability is likely high enough to sustain high metabolic rates. The

period when DOC contributes substantially to bacterial biomass seems to last longer at the more eutrophic site BB (November to May) compared to the restored site GM (November to March). Hence, on annual basis, consumption of allochthonous carbon may be rather similar, possibly as a result of larger bacterial standing stocks.

Conclusions

In the two sub basins of Lake Naarden, $\delta^{13}\text{C}$ values of individual phytoplankton PLFAs and $\text{CO}_{2(\text{aq})}$ differed by up to 11.3‰ within the same month, but showed similar seasonal variation during the sampling period. Differences in $\delta^{13}\text{C}$ values between individual PLFAs were likely related to differences in source organisms and different species-specific fractionation values. Fractionation values between phytoplankton biomass and $\text{CO}_{2(\text{aq})}$ were similar for diatoms and other eukaryotic phytoplankton and differences between sampling sites were small. Highest ϵ values were observed in winter, with values of $23.5 \pm 0.6\text{‰}$ for eukaryotic phytoplankton and $13.6 \pm 0.3\text{‰}$ for cyanobacteria. Lowest ϵ values were observed in summer, with values of $10.5 \pm 0.3\text{‰}$ for eukaryotic phytoplankton and $2.7 \pm 0.1\text{‰}$ for cyanobacteria. Many factors (light, growth rates, etc.) affect phytoplankton fractionation values, but weak positive Pearson correlations between $\epsilon_{\text{CO}_2\text{-biomass}}$ and $p\text{CO}_2$ and general correspondence in trends show highest ϵ values co-occurring with highest $p\text{CO}_2$ (during periods of typically low production rates).

During most months, bacterial biomass derives mainly from phytoplankton (autochthonous) production and dependence on allochthonous carbon is very low. During winter and spring however, bacterial dependence on DOC was considerable, varying between 39% and 77% at site GM, and between 17% and 46% at site BB. The period in which DOC contributed to bacterial biomass however, continued somewhat longer in BB and hence net consumption of allochthonous carbon may be similar or even higher than in GM on an annual basis.

References

- Bade, D. L., and J. J. Cole. 2006. Impact of chemically enhanced diffusion on dissolved inorganic carbon stable isotopes in a fertilized lake. *J. Geophys. Res.* **111**: C01014, 10 p. doi:10.1029/2004JC002684
- Battin, T. J., L. A. Kaplan, S. Findlay, C. S. Hopkins, E. Marti, A. I. Packman, J. D. Newbold, and F. Sabater. 2008. Biophysical controls on organic carbon fluxes in fluvial networks. *Nat. Geosci.* **1**: 95–100. doi:10.1038/ngeo101
- Bontes, B. M., R. Pel, B. W. Ibelings, H. T. S. Boschker, J. J. Middelburg, and E. Van Donk. 2006. The effects of biomanipulation on the biogeochemistry, carbon isotopic composition and pelagic food web relations of a shallow lake. *Biogeosciences* **3**: 69–83. doi:10.5194/bg-3-69-2006
- Bootsma, M. C., A. Barendregt, and J. C. A. Van Alphen. 1999. Effectiveness of reducing external nutrient load entering a eutrophicated shallow lake ecosystem in the Naardermeer nature reserve, The Netherlands. *Biol. Conserv.* **90**: 193–201. doi:10.1016/S0006-3207(99)00027-0
- Boschker, H. T. S., S. C. Nold, P. Wellsbury, D. Bos, W. de Graaf, R. Pel, R. J. Parkes, and T. E. Cappenberg. 1998. Direct linking of microbial populations to specific biogeochemical processes by ^{13}C -labelling of biomarkers. *Nature* **392**: 801–805. doi:10.1038/33900
- Boschker, H. T. S., and J. J. Middelburg. 2002. Stable isotopes and biomarkers in microbial ecology. *FEMS Microbiol. Ecol.* **40**: 85–95. doi:10.1111/j.1574-6941.2002.tb00940.x
- Boschker, H. T. S., T. C. W. Moerdijk-Poortvliet, P. van Breugel, M. Houtekamer, and J. J. Middelburg. 2008. A versatile method for stable carbon isotope analysis of carbohydrates by high-performance liquid chromatography/isotope ratio mass spectrometry. *Rapid Commun. Mass Spectrom.* **22**: 3902–3908. doi:10.1002/rcm.3804
- Brett, M. T. 2014. Are phytoplankton in northern Swedish lakes extremely ^{13}C depleted? *Limnol. Oceanogr.* **59**: 1795–1799. doi:10.4319/lo.2014.59.5.1795
- Brett, M. T., and D. C. Müller-Navarra. 1997. The role of highly unsaturated fatty acids in aquatic foodweb processes. *Freshw. Biol.* **38**: 483–499. doi:10.1046/j.1365-2427.1997.00220.x
- Brett, M. T., M. J. Kainz, S. J. Taipale, and H. Seshan. 2009. Phytoplankton, not allochthonous carbon, sustains herbivorous zooplankton production. *Proc. Natl. Acad. Sci. USA.* **106**: 21197–21201. doi:10.1073/pnas.0904129106
- Burkhardt, S., U. Riesebell, and I. Zondervan. 1999. Stable carbon isotope fractionation by marine phytoplankton in response to daylength, growth rate, and CO_2 availability. *Mar. Ecol. Prog. Ser.* **184**: 31–41. doi:10.3354/meps184031
- Buser, H. R., H. Arn, P. Guerin, and S. Rauscher. 1983. Determination of double bond position in mono-unsaturated acetates by mass spectrometry of dimethyl disulfide adducts. *Anal. Chem.* **55**: 818–822. doi:10.1021/ac00257a003
- Cole, J. J., S. Findlay, and M. L. Pace. 1988. Bacterial production in fresh and saltwater ecosystems: A cross-system overview. *Mar. Ecol. Prog. Ser.* **43**: 1–10. doi:10.3354/meps043001
- Cole, J. J., N. F. Caraco, G. W. Kling, and T. K. Kratz. 1994. Carbon dioxide supersaturation in the surface waters of lakes. *Science* **265**: 1568–1570. doi:10.1126/science.265.5178.1568
- Cole, J. J., S. R. Carpenter, M. L. Pace, C. van de Bogert, J. F. Kitchell, and J. R. Hodgson. 2006. Differential support of lake food webs by three types of terrestrial organic carbon. *Ecol. Lett.* **9**: 558–568. doi:10.1111/j.1461-0248.2006.00898.x
- Cole, J. J., and others. 2007. Plumbing the global carbon cycle: Integrating inland waters into the terrestrial carbon budget. *Ecosystems* **10**: 171–184. doi:10.1007/s10021-006-9013-8
- Cole, J. J., and Y. T. Prairie. 2009. Dissolved CO_2 , p. 30–34. *In* G. E. Likens [ed.], *Encyclopedia of inland waters*. Elsevier.

- Cole, J. J., S. R. Carpenter, J. F. Kitchell, M. L. Pace, C. T. Solomon, and B. C. Weidel. 2011. Strong evidence for terrestrial support of zooplankton in small lakes based on stable isotopes of carbon, nitrogen, and hydrogen. *Proc. Natl. Acad. Sci. USA.* **108**: 1975–1980. doi:10.1073/pnas.1012807108
- Coloso, J. J., J. J. Cole, and M. L. Pace. 2011. Difficulty in discerning drivers of lake ecosystem metabolism with high-frequency data. *Ecosystems* **14**: 935–948. doi:10.1007/s10021-011-9455-5
- De Kluijver, A., K. Soetaert, K. G. Schulz, U. Riesebeck, R. G. J. Bellerby, and J. J. Middelburg. 2010. Phytoplankton-bacteria coupling under elevated CO₂ levels: A stable isotope labelling study. *Biogeosciences* **7**: 3783–3797. doi:10.5194/bg-7-3783-2010
- De Kluijver, A., P. L. Schoon, J. A. Downing, S. Schouten, and J. J. Middelburg. 2014. Stable carbon isotope biogeochemistry of lakes along a trophic gradient. *Biogeosciences* **11**: 6265–6276. doi:10.5194/bg-11-6265-2014
- De Kluijver, A., J. Ning, Z. Liu, E. Jeppesen, R. D. Gulati, and J. J. Middelburg. 2015. Macrophytes and periphyton carbon subsidies to bacterioplankton and zooplankton in a shallow eutrophic lake in tropical China. *Limnol. Oceanogr.* **60**: 375–385. doi:10.1002/lno.10040
- Degens, E. T., R. R. L. Guillard, W. M. Sackett, and J. A. Helleburst. 1968. Metabolic fractionation of carbon isotopes in marine plankton: Temperature and respiration experiments. *Deep-Sea Res. Oceanogr. Abstr.* **15**: 1–9. doi:10.1016/0011-7471(68)90024-7
- Dickson, L., I. D. Bull, P. J. Gates, and R. P. Evershed. 2009. A simple modification of a silicic acid lipid fractionation protocol to eliminate free fatty acids from glycolipid and phospholipid fractions. *J. Microbiol. Methods* **78**: 249–254. doi:10.1016/j.mimet.2009.05.014
- Dijkman, N. A., and J. C. Kromkamp. 2006. Phospholipid-derived fatty acids as chemotaxonomic markers for phytoplankton: Application for inferring phytoplankton composition. *Mar. Ecol. Prog. Ser.* **324**: 113–125. doi:10.3354/meps324113
- Farquhar, G. D., J. R. Ehlinger, and K. T. Hubick. 1989. Carbon isotope discrimination and photosynthesis. *Annu. Rev. Plant Physiol. Plant Mol. Biol.* **40**: 503–537. doi:10.1146/annurev.pp.40.060189.002443
- Feeley, J. K. 1999. Photosynthetic pathway diversity in a seasonal pool community. *Funct. Ecol.* **13**: 106–118. doi:10.1046/j.1365-2435.1999.00294.x
- Finlay, F. C. 2004. Patterns and controls of lotic algal stable carbon isotope ratios. *Limnol. Oceanogr.* **49**: 850–861. doi:10.4319/lo.2004.49.3.0850
- Fry, B., C. S. J. Hopkinson, A. Nolin, and S. C. Wainwright. 1998. ¹³C/¹²C composition of marine dissolved organic carbon. *Chem. Geol.* **152**: 113–118. doi:10.1016/S0009-2541(98)00100-4
- Grey, J., and R. I. Jones. 2001. Seasonal changes in the importance of the source of organic matter to the diet of zooplankton in Loch Ness, as indicated by stable isotope analysis. *Limnol. Oceanogr.* **46**: 505–513. doi:10.4319/lo.2001.46.3.0505
- Gugger, M., C. Lyra, I. Suominen, I. Tsitko, J. F. Humbert, M. S. Salkinoja-Salonen, and K. Sivonen. 2002. Cellular fatty acids as chemotaxonomic markers of the genera *Anabaena*, *Aphanizomenon*, *Microcystis*, *Nostoc* and *Planktothrix* (cyanobacteria). *Int. J. Syst. Evol. Microbiol.* **52**: 1007–1015. doi:10.1099/00207713-52-3-1007
- Haack, S. K., H. Garchow, D. A. Odelson, L. J. Forney, and M. J. Klug. 1994. Accuracy, reproducibility, and interpretation of fatty acid methyl ester profiles of model bacterial communities. *Appl. Environ. Microbiol.* **60**: 2483–2493.
- Harvey, H. R., R. D. Fallom, and J. S. Patton. 1986. The effect of organic matter and oxygen on the degradation of bacterial membrane lipids in marine sediments. *Geochim. Cosmochim. Acta* **50**: 795–805. doi:10.1016/0016-7037(86)90355-8
- Hayes, J. M. 2001. Fractionation of carbon and hydrogen isotopes in biosynthetic processes, p. 225–277. In J. W. Valley and D. Cole [eds.], *Stable isotope geochemistry, reviews in mineralogy & geochemistry*. V. **43**. Mineralogical Society of America.
- Hoins, M., D. B. Van de Waal, T. Eberlein, G. J. Reichart, B. Rost, and A. Sluijs. 2015. Stable carbon isotope fractionation of organic cyst-forming dinoflagellates: Evaluating the potential for a CO₂ proxy. *Geochim. Cosmochim. Acta* **160**: 267–276. doi:10.1016/j.gca.2015.04.001
- Hoins, M., T. Eberlein, D. B. Van de Waal, A. Sluijs, G. J. Reichart, and B. Rost. 2016. CO₂-dependent carbon isotope fractionation in dinoflagellates relates to their inorganic carbon fluxes. *J. Exp. Mar. Biol. Ecol.* **481**: 9–14. doi:10.1016/j.jembe.2016.04.001
- Kaneda, T. 1991. Iso-fatty and anteiso-fatty acids in bacteria – biosynthesis, function and taxonomic significance. *Microbiol. Rev.* **55**: 288–302.
- Keller, K., and F. M. M. Morel. 1999. A model of carbon isotopic fractionation and active carbon uptake in phytoplankton. *Mar. Ecol. Prog. Ser.* **182**: 295–298. doi:10.3354/meps182295
- Keough, J. E., M. Sierzen, and C. Hagley. 1996. Analysis of a Lake Superior coastal food web with stable isotopes. *Limnol. Oceanogr.* **41**: 136–146. doi:10.4319/lo.1996.41.1.0136
- Kling, G. W., B. Fry, and W. J. O'Brien. 1992. Stable isotopes and planktonic trophic structures in Arctic lakes. *Ecology* **73**: 561–566. doi:10.2307/1940762
- Laws, E. A., B. N. Popp, R. R. Bidigare, M. C. Kennicutt, and S. A. Macko. 1995. Dependence of phytoplankton carbon isotopic composition on growth rate and (CO₂)_{aq}: Theoretical considerations and experimental results. *Geochim. Cosmochim. Acta* **59**: 1131–1138. doi:10.1016/0016-7037(95)00030-4

- Lucas, W. J., and J. A. Berry. 1985. Inorganic carbon transport in aquatic photosynthetic organisms. *Physiol. Plant.* **65**: 539–543. doi:10.1111/j.1399-3054.1985.tb08687.x
- Marty, J., and D. Planas. 2008. Comparison of methods to determine algal delta C-13 in freshwater. *Limnol. Oceanogr.-Meth.* **6**: 51–63. doi:10.4319/lom.2008.6.51
- McDonald, C. P., E. G. Stets, R. G. Striegl, and D. Butman. 2013. Inorganic carbon loading as a primary driver of dissolved carbon dioxide concentrations in the lakes and reservoirs of the contiguous United States. *Global Biogeochem. Cycles* **27**: 285–295. doi:10.1002/gbc.20032
- Middelburg, J. J. 2014. Stable isotopes dissect aquatic food webs from the top to the bottom. *Biogeosciences* **11**: 2357–2371. doi:10.5194/bg-11-2357-2014
- Middelburg, J. J., C. Barranguet, H. T. S. Boschker, P. M. J. Herman, T. Moens, and C. H. R. Heip. 2000. The fate of intertidal microphytobenthos carbon: An in situ ^{13}C -labeling study. *Limnol. Oceanogr.* **45**: 1224–1234. doi:10.4319/lo.2000.45.6.1224
- Mizutani, H., and E. Wada. 1982. Effects of high atmospheric CO_2 on $\delta^{13}\text{C}$ of algae. *Orig. Life* **12**: 377–390. doi:10.1007/BF00927070
- Montagnes, D. J., J. A. Berges, P. J. Harrison, and F. J. R. Taylor. 1994. Estimating carbon, nitrogen, protein, and chlorophyll a from volume in marine phytoplankton. *Limnol. Oceanogr.* **39**: 1044–1060. doi:10.4319/lo.1994.39.5.1044
- Mook, W. G., J. C. Bommerson, and W. H. Staverman. 1974. Carbon isotope fractionation between dissolved bicarbonate and gaseous carbon dioxide. *Earth Planet. Sci. Lett.* **22**: 169–176. doi:10.1016/0012-821X(74)90078-8
- Morana, C., and others. 2015. Biogeochemistry of a large and deep tropical lake (Lake Kivu, East Africa: Insights from a stable isotope study covering an annual cycle. *Biogeosciences* **12**: 4953–4963. doi:10.5194/bg-12-4953-2015
- O'Leary, M. H. 1988. Carbon isotopes in photosynthesis. *BioScience* **38**: 325–336.
- Pace, M. L., and others. 2004. Whole-lake carbon-13 additions reveal terrestrial support of aquatic food webs. *Nature* **427**: 240–243. doi:10.1038/nature02227
- Pace, M. L., and others. 2007. Does terrestrial organic carbon subsidize the planktonic food web in a clear-water lake? *Limnol. Oceanogr.* **52**: 2177–2189. doi:10.4319/lo.2007.52.5.2177
- Pel, R., V. Floris, and H. van Hoogveld. 2004. Analysis of planktonic community structure and trophic interactions using refined isotopic signatures determined by combining fluorescence-activated cell sorting and isotope-ratio mass spectrometry. *Freshw. Biol.* **49**: 546–562. doi:10.1111/j.1365-2427.2004.01212.x
- Peterson, B. J., and B. Fry. 1987. Stable isotopes in ecosystem studies. *Annu. Rev. Ecol. Syst.* **18**: 293–320. doi:10.1146/annurev.es.18.110187.001453
- Popp, B. N., E. A. Laws, R. R. Bidigare, J. E. Dore, K. L. Hanson, and S. G. Wakeham. 1998. Effect of phytoplankton cell geometry on carbon isotopic fractionation. *Geochim. Cosmochim. Acta* **62**: 69–77. doi:10.1016/S0016-7037(97)00333-5
- Rost, B., I. Zondervan, and U. Riesebeck. 2002. Light-dependent carbon isotope fractionation in the coccolithophorid *Emiliania huxleyi*. *Limnol. Oceanogr.* **47**: 120–128. doi:10.4319/lo.2002.47.1.0120
- Rütters, H., H. Sass, H. Cypionka, and J. Rullkötter. 2002. Phospholipid analysis as a tool to study complex microbial communities in marine sediments. *J. Microbiol. Methods* **48**: 149–160. doi:10.1016/S0167-7012(01)00319-0
- Schouten, S., W. Breteler, P. Blokker, N. Schogt, W. I. C. Rijpstra, K. Grice, M. Baas, and J. S. Sinninghe Damsté. 1998. Biosynthetic effects on the stable carbon isotopic compositions of algal lipids: Implications for deciphering the carbon isotopic biomarker record. *Geochim. Cosmochim. Acta* **62**: 1397–1406. doi:10.1016/S0016-7037(98)00076-3
- Sessions, A. L. 2006. Isotope-ratio detection for gas chromatography. *J. Sep. Sci.* **29**: 1946–1961. doi:10.1002/jssc.200600002
- Staehr, P. A., and K. Sand-Jensen. 2007. Temporal dynamics and regulation of lake metabolism. *Limnol. Oceanogr.* **52**: 108–120. doi:10.4319/lo.2007.52.1.0108
- Staehr, P. A., D. Bade, M. C. van de Bogert, G. R. Koch, C. Williamson, P. Hanson, J. J. Cole, and T. K. Kratz. 2010. Lake metabolism and the diel oxygen technique: State of the science. *Limnol. Oceanogr.* **8**: 628–644. doi:10.4319/lom.2010.8.0628
- Taipale, S. J., U. Strandberg, E. Peltomaa, A. W. E. Galloway, A. Ojala, and M. T. Brett. 2013. Fatty acid composition as biomarkers of freshwater microalgae: Analysis of 37 strains of microalgae in 22 genera and in seven classes. *Aquat. Microb. Ecol.* **71**: 165–178. doi:10.3354/ame01671
- Taipale, S. J., E. Peltomaa, M. Hiltunen, R. I. Jones, M. W. Hahn, C. Biasi, and M. T. Brett. 2015. Inferring phytoplankton, terrestrial plant and bacteria bulk $\delta^{13}\text{C}$ values from compound specific analyses of lipids and fatty acids. *PLoS One* **10**: e0133974. doi:10.1371/journal.pone.0133974
- Taipale, S. J., A. W. E. Galloway, S. L. Aalto, K. K. Kahilainen, U. Strandberg, and P. Kankaala. 2016a. Terrestrial carbohydrates support freshwater zooplankton during phytoplankton deficiency. *Sci. Rep.* **6**: 30897. doi:10.1038/srep30897
- Taipale, S. J., K. Vuorio, M. T. Brett, E. Peltomaa, M. Hiltunen, and P. Kankaala. 2016b. Lake zooplankton $\delta^{13}\text{C}$ values are strongly correlated with the $\delta^{13}\text{C}$ values of distinct phytoplankton taxa. *Ecosphere* **7**: e01392. doi:10.1002/ecs2.1392
- Tranvik, L. J., and others. 2009. Lakes and reservoirs as regulators of carbon cycling and climate. *Limnol. Oceanogr.* **65**: 2298–2314. doi:10.4319/lo.2009.54.6_part_2.2298
- Van Breugel, Y., S. Schouten, M. Paetzel, and J. S. Sinninghe Damsté. 2006. Seasonal variation in the stable carbon isotopic composition of algal lipids in a shallow anoxic fjord: Evaluation of the effect of recycling of respired CO_2 on

- the $\delta^{13}\text{C}$ of organic matter. *Am. J. Sci.* **306**: 367–387. doi: [10.2475/05.2006.03](https://doi.org/10.2475/05.2006.03)
- Van den Meersche, K., P. van Rijswijk, K. Soetaert, and J. J. Middelburg. 2009. Autochthonous and allochthonous contributions to mesozooplankton diet in a tidal river and estuary: Integrating carbon isotope and fatty acid constraints. *Limnol. Oceanogr.* **54**: 62–74. doi:[10.4319/lo.2009.54.1.0062](https://doi.org/10.4319/lo.2009.54.1.0062)
- Van Ee, G. 2007. Naardermeer op weg naar volledig herstel. *In* *Diatomededelingen* 31. Nederlands-Vlaamse Kring van Diatomisten.
- Vermaas, W. F. J. 2001. Photosynthesis and respiration in cyanobacteria, p. 245–251. *In* Anonymous [ed.], *Encyclopedia of life sciences*. Nature Publishing Group.
- Vink, J. P. M. 2013. Flexibel peilbeheer Naardermeer: Effecten op waterkwaliteit, in. *Deltares Report* 1204348-000, the Netherlands.
- White, D. C., W. M. David, J. S. Nickels, J. D. King, and R. J. Bobbie. 1979. Determination of the sedimentary microbial biomass by extractible lipid phosphate. *Oecologia* **40**: 51–62. doi:[10.1007/BF00388810](https://doi.org/10.1007/BF00388810)
- Wilson, D. E. 1979. The influence of humic compounds on titrimetric determinations of organic carbon in freshwater. *Arch. Hydrobiol.* **87**: 379–384. doi:[10.1002/ecs2.1392](https://doi.org/10.1002/ecs2.1392)

Acknowledgments

The authors acknowledge Natuurmonumenten, the Society for preservation of nature monuments in The Netherlands, for giving permission for the sampling campaign and especially A. Ouwehand for helpful information and advice. We thank the people at Waterproef for collecting the water samples each month and A.W.E. van Leeuwen-Tolboom and D. B. Kasjaniuk (Utrecht University) for assistance during sampling and technical support. We also thank A. E. van Dijk, G. C. van den Meent-Olieman (Utrecht University), and P. van Breugel (NIOZ Yerseke) for analytical support. Physical and chemical data from 2003 to 2014 were kindly provided by Waternet. We are grateful to three anonymous reviewers and associate editor Anssi Vähätalo for their constructive feedback that helped to improve this manuscript. This research was supported by the Netherlands Organization for Scientific Research (NWO) under grant number 820.02.017 and the Netherlands Earth System Science Center (NESSC).

Conflict of Interest

None declared.

Submitted 24 August 2016
Revised 02 April 2017; 10 May 2017
Accepted 11 May 2017

Associate editor: Anssi Vähätalo